

PROCEEDINGS OF SPIE

SPIDigitalLibrary.org/conference-proceedings-of-spie

Temperature and H₂O concentration measurements for a hybrid rocket motor plume using a single mid-infrared tunable diode laser

Fang, Sihan, Wang, Zezhong, Li, Renjie, Zhang, Zelin, Lin, Xin, et al.

Sihan Fang, Zezhong Wang, Renjie Li, Zelin Zhang, Xin Lin, Fei Li, Xilong Yu, "Temperature and H₂O concentration measurements for a hybrid rocket motor plume using a single mid-infrared tunable diode laser," Proc. SPIE 11567, AOPC 2020: Optical Sensing and Imaging Technology, 115671B (5 November 2020); doi: 10.1117/12.2577499

SPIE.

Event: Applied Optics and Photonics China (AOPC 2020), 2020, Beijing, China

Temperature and H₂O concentration measurements for a hybrid rocket motor plume using a single mid-infrared tunable diode laser

Sihan Fang^{1,2}, Zezhong Wang^{1,2}, Renjie Li^{1,2}, Zelin Zhang^{1,3}, Xin Lin^{1,*}, Fei Li¹, Xilong Yu^{1,2}

¹Institute of Mechanics, Chinese Academy of Sciences, Beijing, 100190, China

²School of Engineering Science, University of Chinese Academy of Sciences, Beijing, 100190, China

³College of Mechatronics Engineering, North University of China, Taiyuan, 030051, China

ABSTRACT

A mid-infrared TDLAS sensor near 2.5 μm was designed for time-resolved measurements of temperature and water vapor partial pressure at the nozzle exit of a laboratory-scale hybrid rocket motor. Several previously used H₂O transitions within 2.4-2.9 μm were thoroughly investigated, and a line-pair containing three transitions (4029.52 cm⁻¹, 4030.51 cm⁻¹ and 4030.73 cm⁻¹) was selected for the optimal overall properties like strong absorbance, sufficient temperature sensitivity, single laser scan, high immunity from the ambient H₂O transitions and low measurement uncertainty affected by temperature over the range of 1500K-2500K. Firing tests were conducted on an oxygen/paraffin-fueled hybrid rocket motor operating at oxygen/fuel ratios (O/Fs) of 3.10, 2.77 and 2.88, corresponding to average combustion pressures of 1.91MPa, 2.09MPa and 2.38MPa. A distributed feedback (DFB) laser tuned repetitively at 2kHz was used as the light source, and simultaneously the transmitted spectra were detected at a 2MHz sampling rate. Finally, a 4.5ms time-scale variations of temperature and H₂O partial pressure were captured by TDLAS sensor. Uncertainty analysis was made in detail based on average temperature (1929.8K, 1926.5K, and 1990.7K) and average H₂O partial pressure (0.237MPa, 0.253MPa, and 0.285MPa), leading to temperature uncertainty of around 2.24% and partial pressure uncertainties of around 3.80%, 3.79% and 4.04% respectively. The time-resolved measurement results and small measurement uncertainties indicate that TDLAS has the potential to evaluate the combustion performance of hybrid rocket motor.

Keywords: Tunable diode laser absorption spectroscopy (TDLAS), hybrid rocket motor, nozzle exit, water vapor, temperature, concentration

*Corresponding author.

E-mail address: linxin_bit@163.com (X.Lin)

1. INTRODUCTION

Hybrid rocket motors, generally comprising solid fuel and liquid oxidizer, are promising for future space missions. Although hybrid rocket motors have advantages in higher theoretical specific impulse, higher safety and lower cost compared with solid- or liquid- propulsion motor, suboptimal performances in low regression rate and combustion efficiency continue to hinder hybrid rocket motor development.

In recent years, optimization in solid fuel structure^[1] and composition^[2] have encouraged further investigation of hybrid rocket motor, this requires particular need to characterize the combustion process. Traditional measurements of global parameters like chamber pressure or total mass flow rate are typically used to evaluate the combustion performances of hybrid rocket motors, however, they can't provide specific information of phase change, flow mixing or heat transfer^[3], these complex physics may relate to low combustion performances. For any thermochemical propulsion system, temperature and species concentration are the two most crucial parameters because they reflect the reaction process and quantify the effects of heat loss. However, notable challenges remain to accurate measurement in harsh flow field with high temperature and pressure of a hybrid rocket motor. Hence, a reliable measurement technology that can provide accurate temperature and H₂O concentration data is needed for further combustion research in hybrid rocket motor.

Tunable diode laser absorption spectroscopy (TDLAS), one of the most advanced optical sensing techniques, exhibits the ability to accurately quantify the temperature and species concentration in real combustion environment. Due to its non-intrusive, sensitive, fast and compact advantages, TDLAS often serves as an effective tool for propulsion systems and experimental facilities such as scramjet and shock tube. In the previous TDLAS measurements, it has been deployed to different devices for flame diagnosis such as premixed flat-flame burner^[4-8], model scramjet combustor^[9] and rotating detonation engine^[10].

In this work, the main goal is to illustrate the ability of TDLAS measurement technology to help investigate the combustion performance of a laboratory-scale hybrid rocket motor. A TDLAS sensor was designed based on direct absorption spectroscopy (DAS), and accurate sensing of temperature and H₂O partial pressure has been conducted on a laboratory-scale oxygen/paraffin-fed hybrid rocket motor. H₂O was targeted as the absorption species because it is a major combustion product of hydrogen or hydrocarbon fuels. A promising line-pair near 2.5 μ m was selected after thorough analysis of several previously used H₂O transitions within 2.4-2.9 μ m. Firing tests were conducted at different oxygen/fuel ratios (O/Fs) and combustion pressures. The time-resolved temperature and H₂O partial pressure at the nozzle exit of hybrid rocket motor were obtained by our TDLAS sensor. Line-pair selection and sensor configuration are detailed and measurement results are presented herein.

2. ABSORPTION SPECTROSCOPY FUNDAMENTALS

2.1 Laser absorption

TDLAS exploits the absorption of radiation caused by its interaction with gases to quantify the temperature and species concentration. Although the theory of direct absorption laser spectroscopy was well-discussed in previous studies^[11],

^{12]}, a brief description is shown here for better understanding of the sensor design presented below.

When a laser beam passes through a gas medium, the absorption of monochromatic light is described by the Beer-Lambert relation:

$$(I_t/I_0)_\nu = \exp(-k_\nu \cdot L) \quad (1)$$

where $I_0(\nu)$ represents the incident laser intensity at wavenumber ν cm^{-1} , and I_t is the corresponding transmitted laser intensity, L [cm] is the optical length, and k_ν [cm^{-1}] is the spectral absorption coefficient, which can be expressed as:

$$k_\nu = PX_{abs} \cdot S_i(T) \cdot \phi(\nu) \quad (2)$$

Where P [atm] is the static pressure, X_{abs} is the mole fraction of a specific absorbing species, $S_i(T)$ [$\text{cm}^2\text{atm}^{-1}$] is the linestrength of transition i , it is the function of gas temperature T [K], and is determined by the following expression:

$$S(T) = S(T_0) \frac{Q(T_0)}{Q(T)} \left(\frac{T_0}{T} \right) \exp \left[-\frac{hcE^*}{k} \left(\frac{1}{T} - \frac{1}{T_0} \right) \right] \frac{\left[1 - \exp \left(\frac{-h\nu_0}{kT} \right) \right]}{\left[1 - \exp \left(\frac{-h\nu_0}{kT_0} \right) \right]} \quad (3)$$

Where T_0 [K] is the reference temperature (generally 296K), ν_0 [cm^{-1}] is the line-center frequency of the transition, h [J·s] is Planck's constant, c [cm/s] is the speed of light, E^* [cm^{-1}] is the lower state energy of the quantum transition, k [J/K] is Boltzmann's constant, $Q(T)$ is the temperature-dependent partition function of the absorbing species, which indicates the number fraction of the lower state species at temperature T . The value of E^* , $S(T_0)$ and $Q(T)$ can be taken from HITRAN database^[13]. ϕ [cm] is the line-shape function, and the area underneath ϕ can be normalized to unity:

$$\int \phi(\nu) d\nu \equiv 1 \quad (4)$$

Then the integrated absorbance A_i [cm^{-1}] of transition i for uniform flow field can be obtained by:

$$A_i = \int_{-\infty}^{+\infty} k_\nu L d\nu = PX_{abs} \cdot S_i(T) \cdot L \quad (5)$$

If a pair of monochromatic light is adapted, the path-averaged temperature can be determined by comparing the A_i of the two transitions which have different temperature properties. Then the integrated area ratio R is obtained:

$$R = \frac{A_1}{A_2} = \frac{S_1}{S_2} \quad (6)$$

Because these two transitions are obtained with the same partial pressure PX_{abs} and same optical length L , the ratio of the integrals is equal to the ratio of linestrength. Combined with the expression of linestrength S_i , the area ratio R is expressed as:

$$R = \frac{S_1(T_0)}{S_2(T_0)} \exp \left[-\left(\frac{hc}{k} \right) (E_1^* - E_2^*) \left(\frac{1}{T} - \frac{1}{T_0} \right) \right] \quad (7)$$

Noting that the area ratio R is only dependent on gas temperature T , the R - T curve can be simulated for a particular line-pair. Hence, if given an experimental value of R , the gas temperature T can be obtained. Then, the species partial pressure PX_{abs} is inferred from Eq.5,

$$PX_{abs} = \frac{A_i}{S_i(T) \cdot L} \quad (8)$$

Since gas temperature T is directly determined by ratio R , γ is defined as the unit change in R per unit change in temperature T to demonstrate the temperature sensitivity of a specific line-pair:

$$\chi_T = \frac{dR/R}{dT/T} = \frac{hc}{k} \left| \frac{E_1^* - E_2^*}{T} \right| = \frac{hc}{k} \frac{|\Delta E^*|}{T} \quad (9)$$

2.2 H₂O line-pair selection

Line selection is an important procedure in TDLAS sensor design as properties of absorption lines greatly influence the sensor performance. Since noise background becomes significant in harsh environment, stronger linestrength is needed to provide higher signal-to-noise ratio (SNR) which ensures measurement accuracy and precision. Fundamental absorption vibration bands near 2.5 μ m have stronger linestrength than overtone and combination band transitions^[9], hence, we chose to investigate the wavelength of H₂O transitions within 2.4-2.9 μ m. In this work, the peak absorbance of selected H₂O lines should be over 0.1%^[4]. Additionally, linestrengths of CO, CO₂ and H₂O within the near and mid-infrared region were simulated at 1500K based on HITRAN 2016 database^[13] and HITEMP 2010 database^[14]. Fig.1 shows that H₂O transitions near 2.5 μ m is free of CO₂ interference and have manageable interferences from CO. The selected transitions should also be free of neighboring interference transitions, no strong transition lines within $\pm 0.3\text{cm}^{-1}$ is expected^[5, 12]. Temperature sensitivity χ_T is crucial to successfully measure the gas temperature. Generally, R is required to be larger than 1, leading to a minimum difference in lower state of 1000 cm^{-1} since our interest scale of combustion temperature ranges from 1500K to 2500K.

According to the aforementioned criteria, several previously used H₂O transitions^[4-10, 15] within 2.4-2.9 μ m were thoroughly investigated, four potential line-pairs were obtained and pertinent parameters are listed in Table 1. Segments of the simulated H₂O absorption spectra for these four line-pairs are plotted in Fig.2. χ_T - T curves of these four line-pairs are shown in Fig.3. Finally, line-pair A is selected for measurements of hybrid rocket motor plume for the following reasons: (1) line pair A has sufficient temperature sensitivity; (2) the linestrength uncertainty affected by temperature uncertainty ΔT is relatively low. Here, the Taylor series method (TSM) of uncertainty propagation^[16] is used and the uncertainty in $S(T)$ can be given by^[17]:

$$\Delta S(T) = S(T) \Delta T \left(-\frac{\partial Q(T)/\partial T}{Q(T)} - \frac{1}{T} + \frac{hcE^*}{k_B T^2} - \frac{hcv_0}{k_B T^2} \cdot \frac{\exp(-hcv_0/k_B T)}{1 - \exp(-hcv_0/k_B T)} \right) \quad (10)$$

Uncertainty analysis is made on two absorption lines of 4029.52 cm^{-1} (line-pair A) and 3920.09 cm^{-1} (line-pair D), fig.4. shows that the linestrength uncertainties of 4029.52 cm^{-1} is much lower than that of 3920.09 cm^{-1} . (3) line-pair A has high immunity from the ambient water vapor. Since a low value of E^* may compromise the accuracy and increase measurement uncertainty^[12], a minimum lower state energy larger than 1500 cm^{-1} was required as shown in Fig.5. (4) line-pair A can be scanned by a single laser scan. Considering the tuning ability of DFB laser, the wavenumber interval of the two absorbing lines should be about 1 cm^{-1} ^[4]. (5) it is noteworthy that line-pair A has three transition lines centered at 4029.52 cm^{-1} , 4030.51 cm^{-1} and 4030.73 cm^{-1} , among which the latter two transitions are close enough to be combined together to improve the SNR and reduce the fitting error.

3. EXPERIMENTAL SETUP

The designed TDLAS sensor was applied to a laboratory-scale hybrid rocket motor, and the sensor configuration is illustrated in this section as shown in Fig.6. A mid-infrared distributed feedback (DFB) diode laser (Nanoplus GmbH) was used as the single-mode laser source and operated near $2.5\mu\text{m}$ to probe transitions near 4029.52 cm^{-1} , 4030.51 cm^{-1} , and 4030.73 cm^{-1} . The DFB laser produced a stable power output of $\sim 10\text{mW}$ and a linewidth less than 3MHz . The laser wavelength was tuned by a linear ramp of injection current at 2kHz using NI-DAQ module, yielding a 0.5ms range of each laser scan. A collimation lens was utilized to focus the laser beam to achieve a diameter of $\sim 0.5\text{mm}$, the collimated light from the laser was then passed through the hybrid rocket motor exit plane. A set of fused silica windows were used to protect optical devices from the high temperature plume. The transmitted light was split into two beams by a beam splitter, one beam was collimated and propagated through a Fabry-Perot interferometer (Thorlabs, Model: SA200-18B, 1.5GHz free space range) for the calibration of the wavelength scanning, and the other beam was detected by the photodetector. Prior to the first photodetector (Thorlabs, PDA10D2), the transmitted laser beam was spectrally filtered to reduce the detected background flame radiation. In addition to the narrow-band filter ($2.5\mu\text{m}$ center wavelength, $\sim 50\text{nm}$ full width at half maximum), an iris was placed in the optical path before the laser beam being refocused on the photodetector. The detected data were sample at 2MHz by NI-DAQ module, which also performed the signal trigger synchronization and data analysis. The control system of the hybrid rocket motor was briefly depicted in Fig.6. Oxygen and pure paraffin were chosen as the propellant, and the motor ignition was remotely conducted by a control system. More information regarding the control system of the hybrid rocket motor was detailed in the work of Wang et al^[18].

4. RESULTS AND DISCUSSION

Three firing tests were conducted on a laboratory-scale hybrid rocket motor operating at combustion pressures of 1.91MPa , 2.09MPa , and 2.38MPa , respectively. This section represents the TDLAS measured results of temperature and H_2O partial pressure at nozzle exit of the motor.

Before further data analysis, 50 sequential raw data scans (25ms) were averaged to remove stochastic noise from the laser and plume fluctuation, which improved SNR of the spectra. A typical averaged scan was shown in Fig.7. The baseline unattenuated laser intensity I_0 was determined by fitting the far wings on both sides of the spectra with a 3-order polynomial, the transmitted laser intensity I was normalized by the fitted baseline. The background signal was also measured in each laser scan and subtracted from the transmitted laser intensity before mathematical data analysis.

The absorption spectra were calculated and fitted by a Voigt profile, a representative fitting results along with the fitting residual were shown in Fig.8. The Voigt fit spectrum was then used to determine integrated absorbance A of the corresponding measurement, spectra data was recorded from the starting point of ignition, and a 4.5s -time-scale history of the integrated absorbance for each firing test was plotted in Fig.9. Based on these integrated absorbance results of three transitions in line-pair A, the path-averaged temperatures were calculated using the two-line ratio while combining absorbance of two transitions at 4030.51cm^{-1} and 4030.73cm^{-1} , H_2O partial pressures were then obtained according to Eq.8 using the integrated absorbance of line 4029.52cm^{-1} . The average temperature results of the three firing tests were 1929.8K ,

1926.5K and 1990.7K, respectively, and the corresponding H₂O partial pressure results were 0.237MPa, 0.253MPa, and 0.285MPa, which were shown in Fig.10 and Fig.11.

For the current TDLAS measurements, detail measurement uncertainty was made based on the Voigt fitting residual and linestrength uncertainty. The Voigt fitting residual (<1%) was obtained from the fitting procedure. Considering the linestrength uncertainty (2%) validated by Goldstein et al^[9], the total uncertainty of measured temperature was 2.24%. The uncertainty in H₂O partial pressure was determined by linestrength uncertainty $\Delta S(T)/S(T)$ given in Eq.10 and the Voigt fitting uncertainty (<1%). For example, when measuring the plume at chamber pressure of 1.91MPa, the linestrength uncertainty was 3.67%, hence, the total uncertainty in H₂O partial pressure was 3.80%. Finally, H₂O partial pressure uncertainties for the three firing tests were 3.80%, 3.79%, and 4.04% respectively. From the uncertainty analysis illustrated above, temperature is found to be the dominant parameter affecting the H₂O partial pressure measurement accuracy. These small uncertainties validate the measurement fidelity in high-temperature plumes of our TDLAS sensor.

5. CONCLUSION

In this work, the design and demonstration of a mid-infrared TDLAS sensor near 2.5 μ m were presented and measurement results for temperature and H₂O partial pressure at nozzle exit of a hybrid rocket motor were reported. Line selection rules were illustrated and used to investigate several previously used transitions of water vapor within 2.4-2.9 μ m. Considering strong absorption strength, isolation from other species, isolation from the nearby transitions and high temperature sensitivity, four potential line-pairs were obtained. Absorption performance of line-pairs A and D were analyzed in detail, and finally line-pair A containing transitions at 4029.52 cm⁻¹, 4030.51 cm⁻¹ and 4030.73 cm⁻¹ was selected for lower linestrength uncertainty affected by temperature, lower interference from the ambient water vapor, single laser scan, higher SNR and lower fitting error.

Temperature and H₂O partial pressure measurements were conducted at the nozzle exit of a laboratory-scale hybrid rocket motor at oxygen/fuel ratios (O/Fs) of 3.10, 2.77 and 2.88, corresponding to average combustion pressures of 1.91MPa, 2.09MPa and 2.38MPa. The 4.5s-time-scale history of temperature and H₂O partial pressure were captured by TDLAS sensor. The average measurement results for three different firing conditions were 1929.8K, 1926.5K and 1990.7K, respectively, and the corresponding H₂O partial pressure results were 0.237MPa, 0.253MPa, and 0.285MPa. Uncertainty analysis were performed to assess TDLAS measurement accuracy. Temperature uncertainty was analyzed to be around 2.24%, leading to concentration uncertainties for the three firing tests of around 3.80%, 3.79% and 4.04% respectively. The time-resolved measurement results and these small uncertainties indicate that TDLAS has the potential to provide high fidelity measurement data for the plume diagnosis of hybrid rocket motor. Further researches are needed to investigate the combustion performances of the hybrid rocket motor using TDLAS measurement technology.

ACKNOWLEDGMENTS

This work was funded by the National Natural Science Foundation of China (No. 11802315 and No. 11927803) and Equipment Pre -research Foundation of National Defense Key Laboratory (No. 6142701190402).

REFERENCE

- [1] Lee, C., Na, Y., Lee, J.-W., et al., "Effect of induced swirl flow on regression rate of hybrid rocket fuel by helical grain configuration", *Aerosp. Sci. Technol.*, 11(1), 68-76 (2007).
- [2] Carmicino, C. and Russo Sorge, A., "Experimental Investigation into the Effect of Solid-Fuel Additives on Hybrid Rocket Performance", *J. Propul. Power*, 31(2), 699-713 (2014).
- [3] Wang, Z., Fu, P. and Chao, X., "Laser Absorption Sensing Systems: Challenges, Modeling, and Design Optimization", *Appl. Sci.*, 9, 2723 (2019).
- [4] Ma, L., Ning, H., Wu, J., et al., "In situ flame temperature measurements using a mid-infrared two-line H₂O laser-absorption thermometry", *Combust. Sci. Technol.*, 190(3), 392-407 (2018).
- [5] Farooq, A., Jeffries, J. B. and Hanson, R. K., "In situ combustion measurements of H₂O and temperature near 2.5 μ m using tunable diode laser absorption", *Meas. Sci. Technol.*, 19(7), 075604 (2008).
- [6] Li, S., Farooq, A. and Hanson, R. K., "H₂O temperature sensor for low-pressure flames using tunable diode laser absorption near 2.9 μ m", *Meas. Sci. Technol.*, 22(12), 125301 (2011).
- [7] Ma, L. H., Lau, L. Y. and Ren, W., "Non-uniform temperature and species concentration measurements in a laminar flame using multi-band infrared absorption spectroscopy", *Appl. Phys. B*, 123(3), 83 (2017).
- [8] Smith, C. H., Goldenstein, C. S. and Hanson, R. K., "A scanned-wavelength-modulation absorption-spectroscopy sensor for temperature and H₂O in low-pressure flames", *Meas. Sci. Technol.*, 25(11), 115501 (2014).
- [9] Goldenstein, C. S., Schultz, I. A., Spearrin, R. M., et al., "Scanned-wavelength-modulation spectroscopy near 2.5 μ m for H₂O and temperature in a hydrocarbon-fueled scramjet combustor", *Appl. Phys. B*, 116(3), 717-727 (2014).
- [10] Peng, W. Y., Cassidy, S. J., Strand, C. L., et al., "Single-ended mid-infrared laser-absorption sensor for time-resolved measurements of water concentration and temperature within the annulus of a rotating detonation engine", *Proc. Combust. Inst.*, 37(2), 1435-1443 (2019).
- [11] Liu, X., "Line-of-sight absorption of H₂O vapor: gas temperature sensing in uniform and nonuniform flows", *Journal*, Volume(Issue), Pages (2006).
- [12] Zhou, X., Jeffries, J. B. and Hanson, R. K., "Development of a fast temperature sensor for combustion gases using a single tunable diode laser", *Appl. Phys. B*, 81(5), 711-722 (2005).
- [13] Gordon, I. E., Rothman, L. S., Hill, C., et al., "The HITRAN2016 molecular spectroscopic database", *J. Quant. Spectrosc. Radiat. Transfer*, 203, 3-69 (2017).
- [14] Rothman, L. S., Gordon, I. E., Barber, R. J., et al., "HITEMP, the high-temperature molecular spectroscopic database", *J. Quant. Spectrosc. Radiat. Transfer*, 111, 2139-2150 (2010).
- [15] Bendana, F. A., Castillo, J. J., Hagström, C. G., et al., "Thermochemical structure of a hybrid rocket reaction layer based on laser absorption tomography", *AIAA Propulsion and Energy 2019 Forum*, AIAA 2019-4337 (2019).
- [16] Hugh W. Coleman, W. G. S., [Experimentation, validation, and uncertainty analysis for engineers], John Wiley & Sons, 79-80 (2018).
- [17] Wei, C., Pineda, D. I., Paxton, L., et al., "Mid-infrared laser absorption tomography for quantitative 2D thermochemistry measurements in premixed jet flames", *Appl. Phys. B*, 124(6), 123 (2018).
- [18] Wang, Z., Lin, X., Li, F., et al., "Combustion performance of a novel hybrid rocket fuel grain with a nested helical structure", *Aerosp. Sci. Technol.*, 97, 105613 (2020).

Fig.1. Simulated linestrengths of CO, H₂O and CO₂ at $T=1500\text{K}$. Parameters of CO₂ and H₂O were taken from HITRAN 2016 database^[13] and parameters of CO were taken from HITEMP 2010 database^[14].

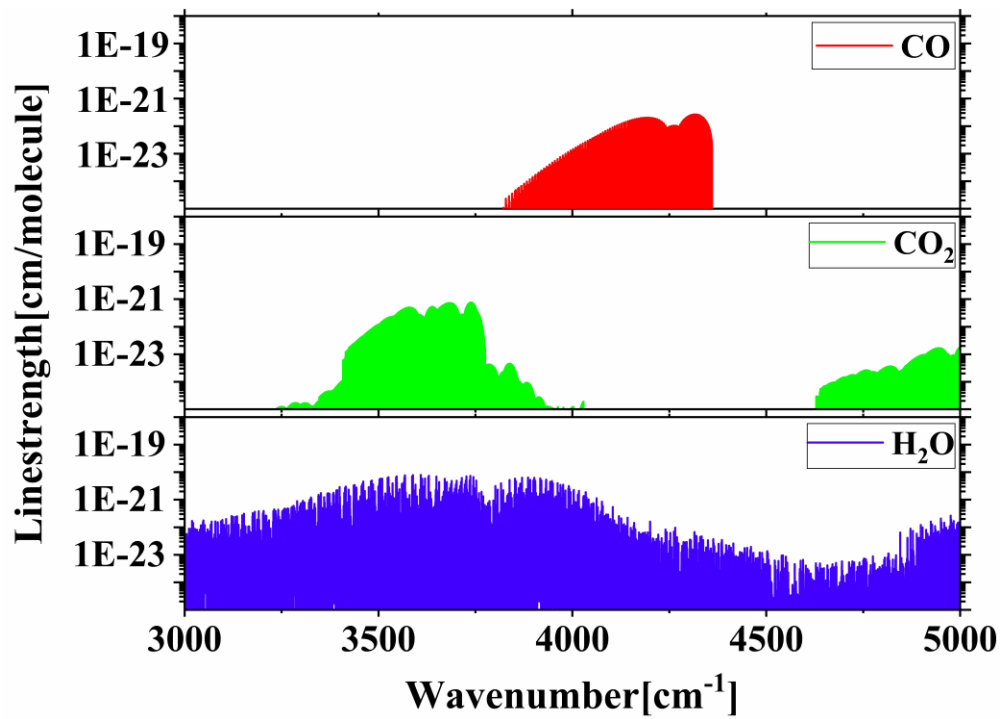


Fig.2. Simulated absorption spectra for the four selected H₂O line pairs in the 2.4-2.9 μ m region based on HITRAN 2016 database^[13]. Simulation condition: $P=1$ atm, 25% H₂O in air, and $L=1$ cm.

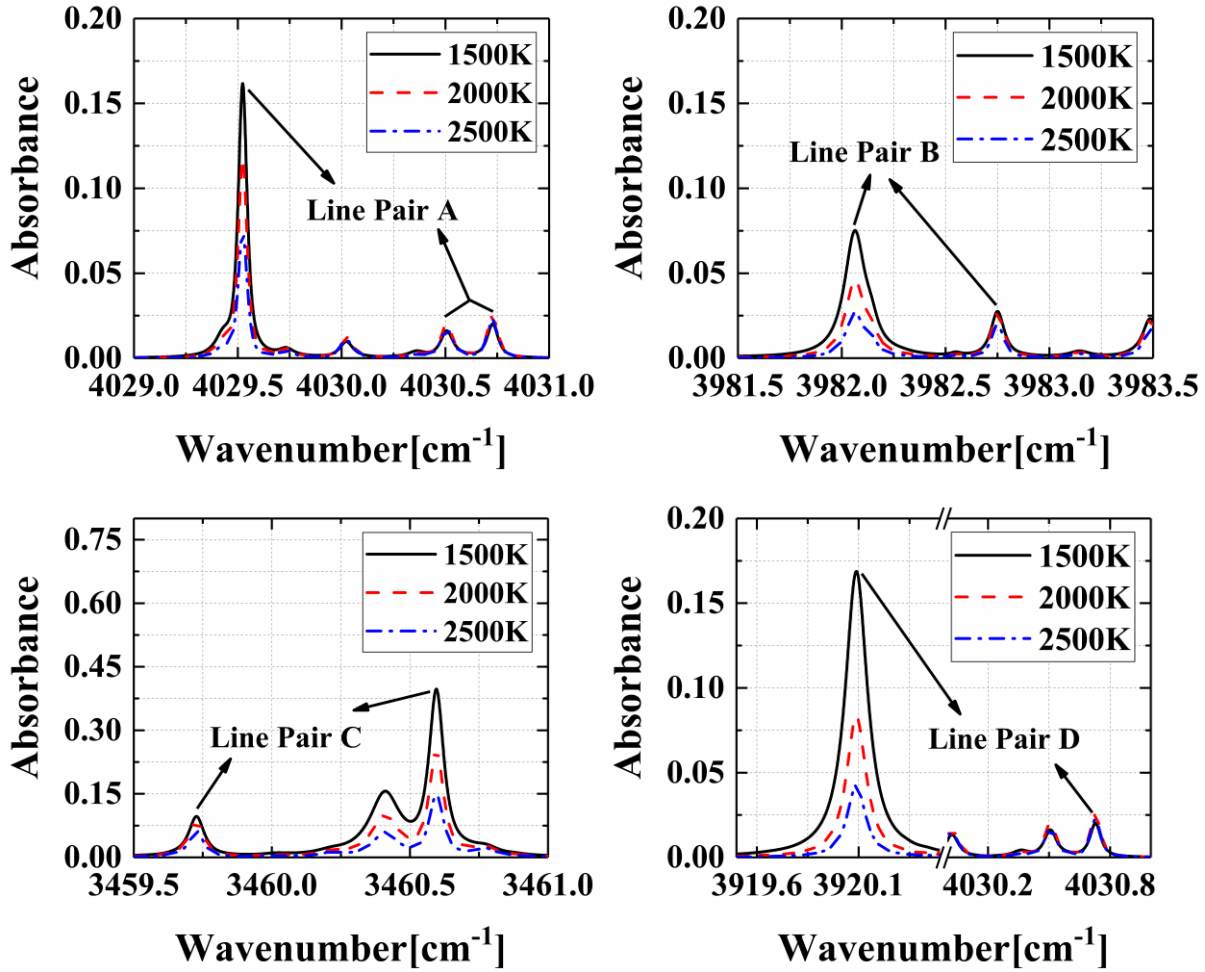


Fig.3. Temperature sensitivity of the four selected line pairs as a function of temperature.

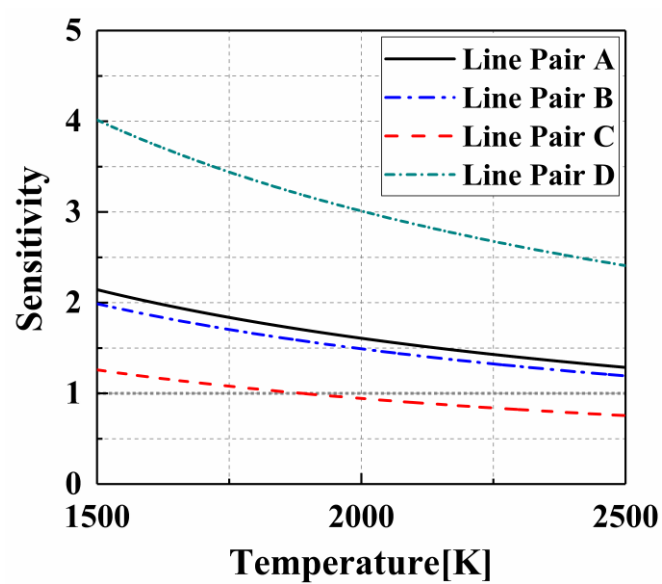


Fig.4. Comparison of linestrength uncertainty affected by temperature of transition lines at 4029.52cm^{-1} (line-pair A) and 3920.09cm^{-1} (line-pair D) when the temperature uncertainty $\Delta T/T$ is of 5%.

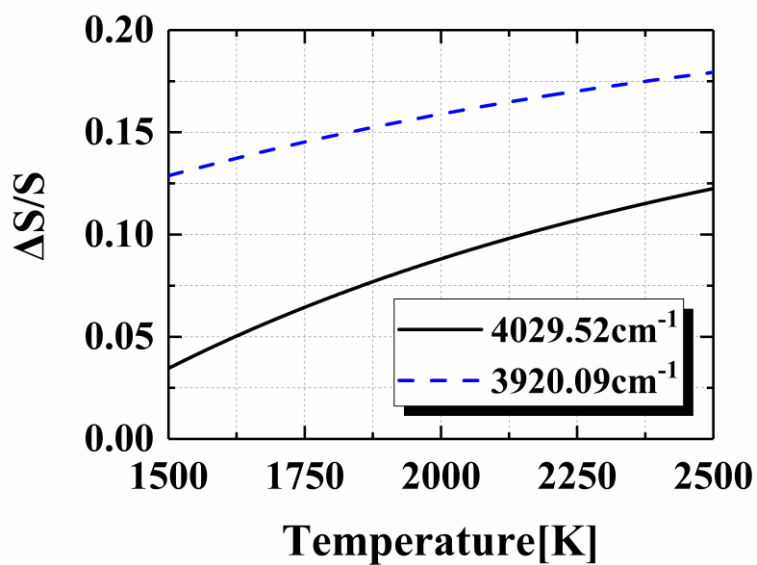


Fig.5. Simulated linestrength ratio $S(T)/S(T_0)$ for different lower state energy E'' of 700cm^{-1} , 900cm^{-1} , 1500cm^{-1} , and 2500cm^{-1} as a function of temperature. Parameters were taken from HITRAN 2016 database^[13].

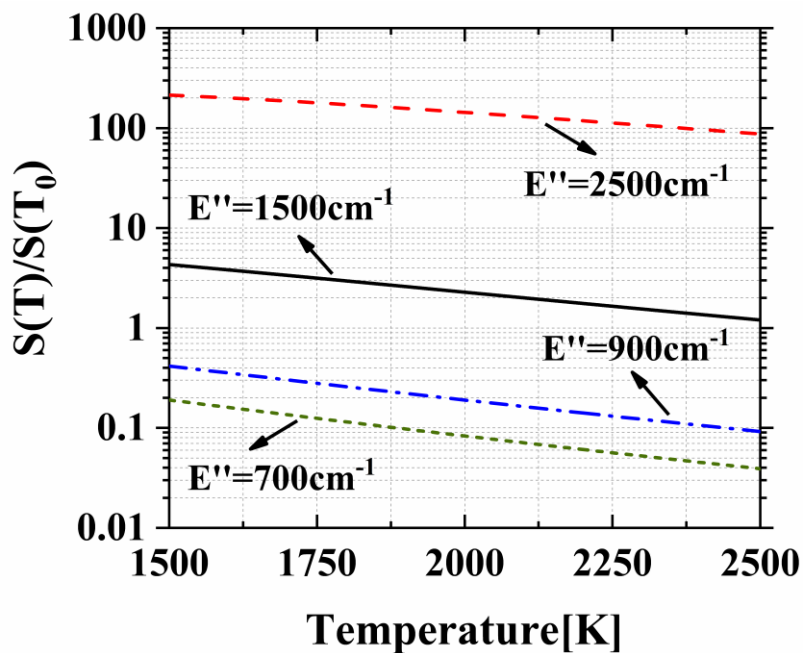


Fig.6. Schematic of TDLAS diagnosis setup used in measurements conducted at the laboratory-scale hybrid rocket motor. Dotted red line emanating from the collimation lens represents the centerline of the detection light. DFB, distributed feedback laser; Fabry-Perot, Fabry-Perot interferometer; PD, photodetector; NBF, narrow-band-pass filter.

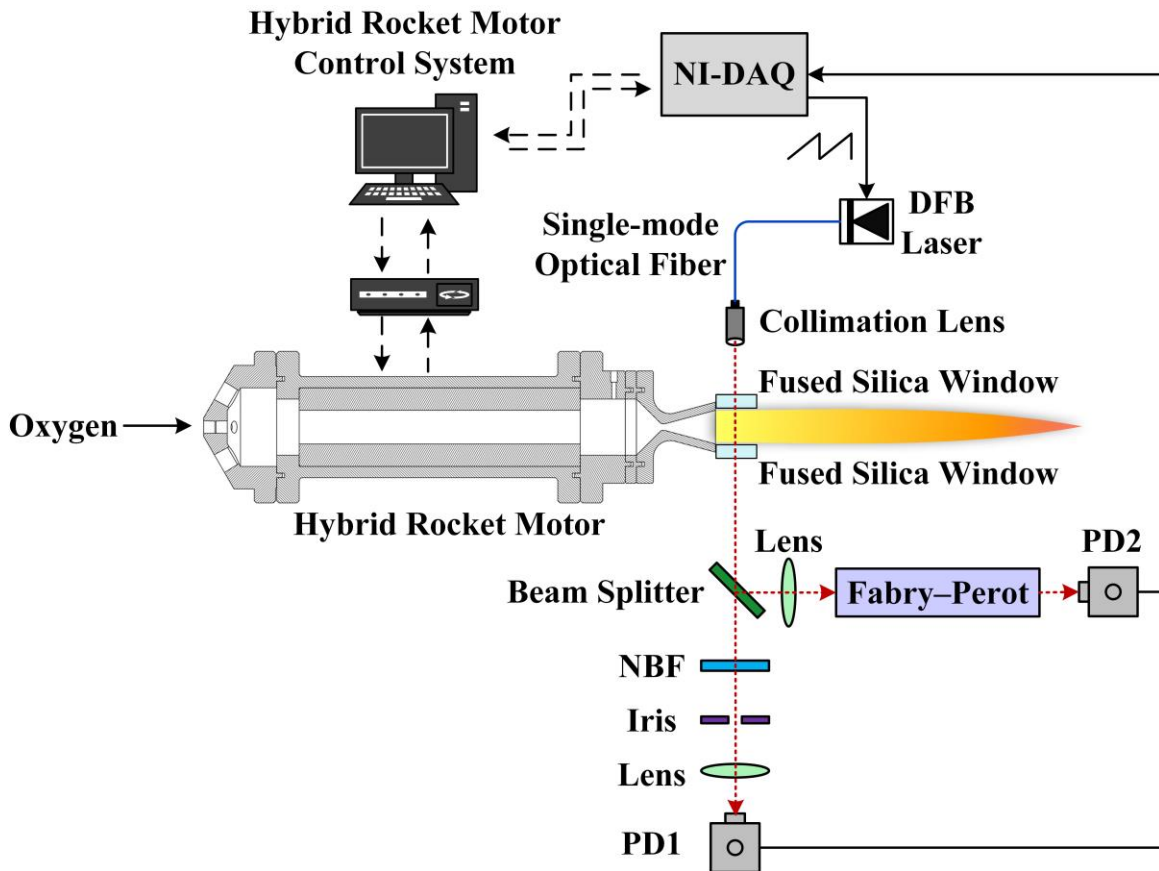


Fig.7. A typical image for the 50-scan averaged sample data in measurements.

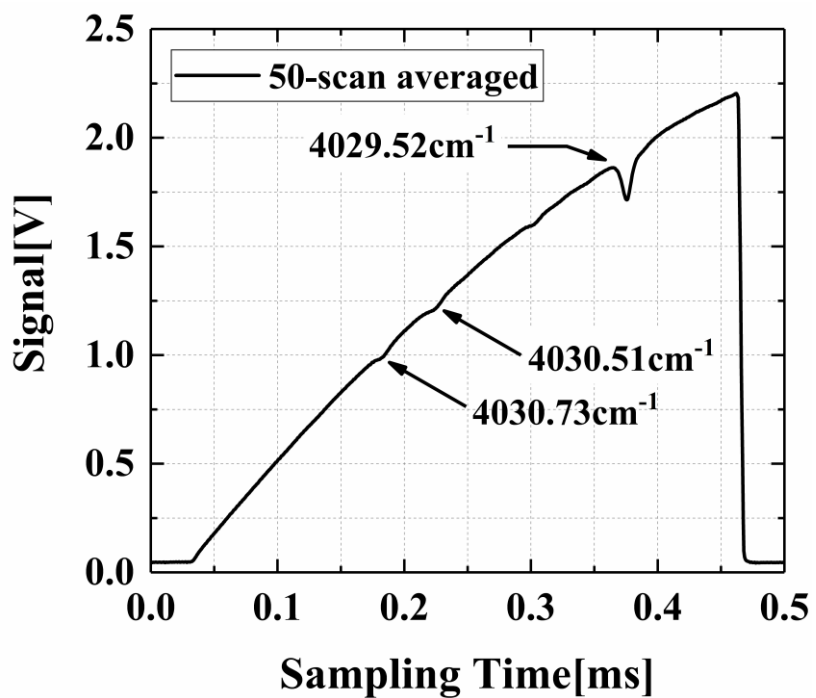


Fig.8. Representative absorption spectra from the experiment (solid line) and its Voigt fitting results (dash line) along with the fitting residuals (bottom).

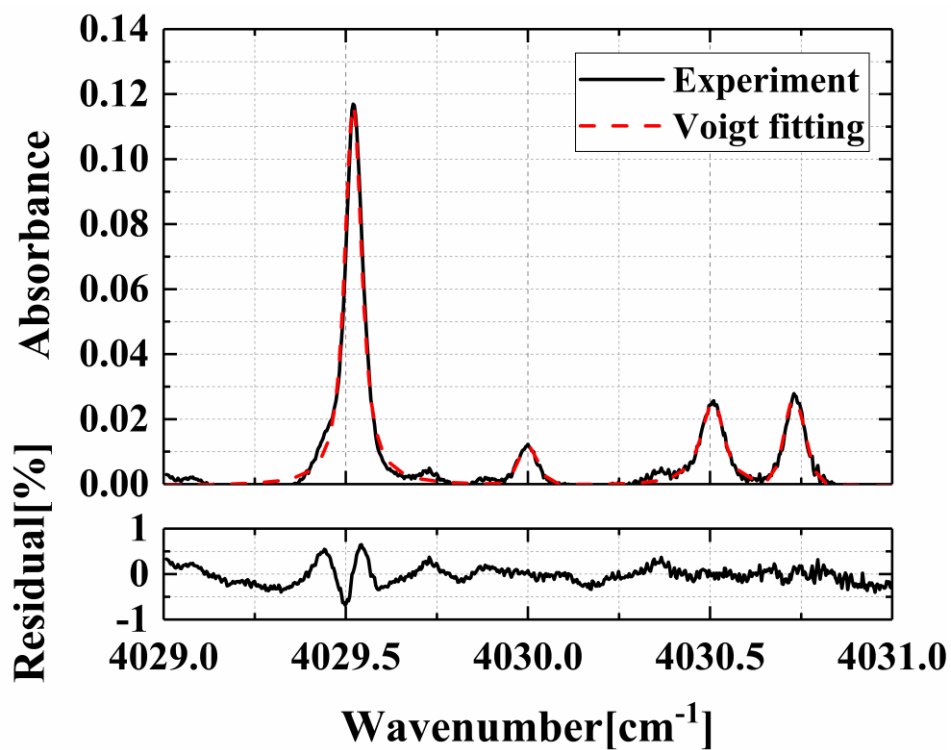


Fig.9. Measured absorbance for the three firing tests.

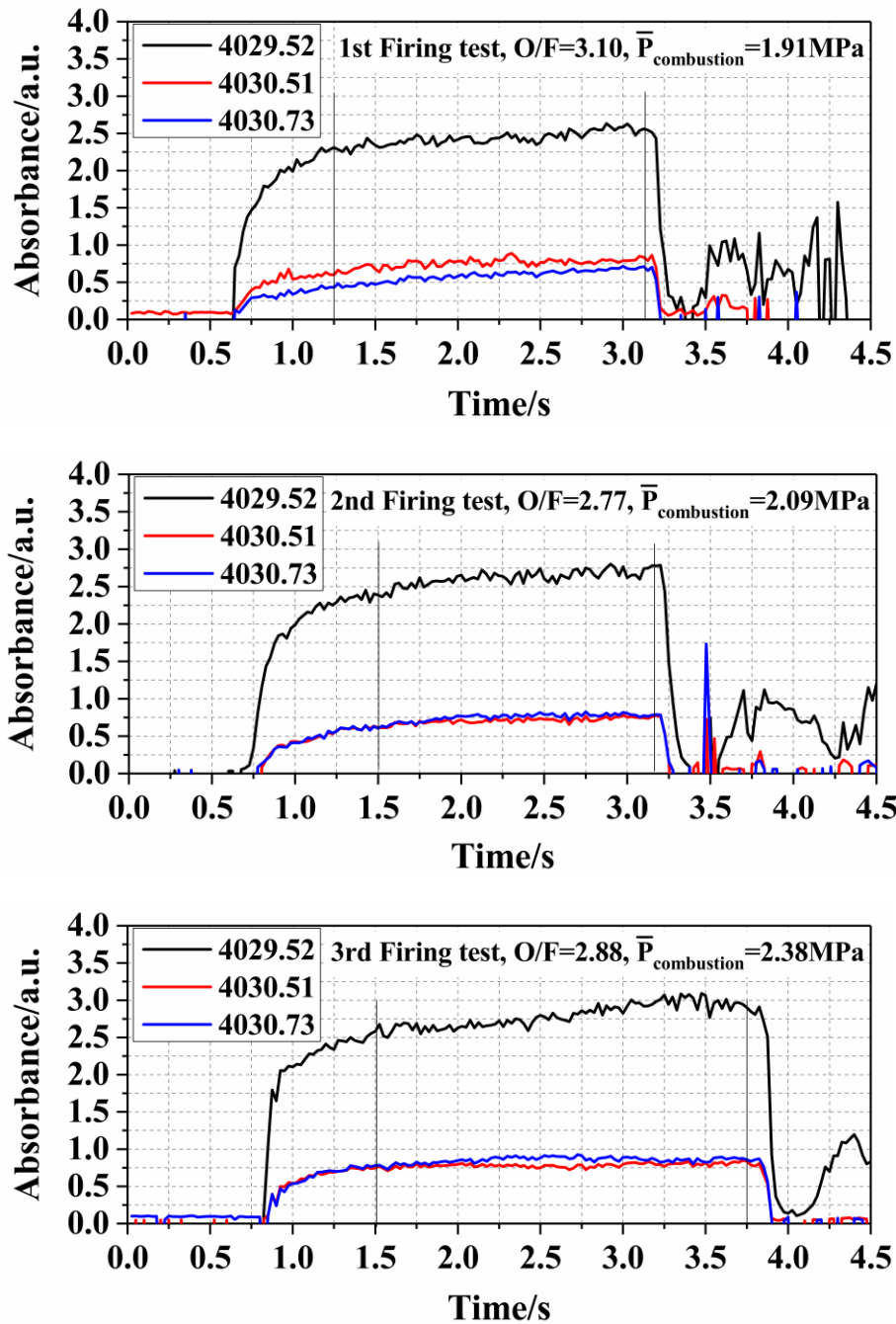


Fig.10. Temperature results for the three firing tests.

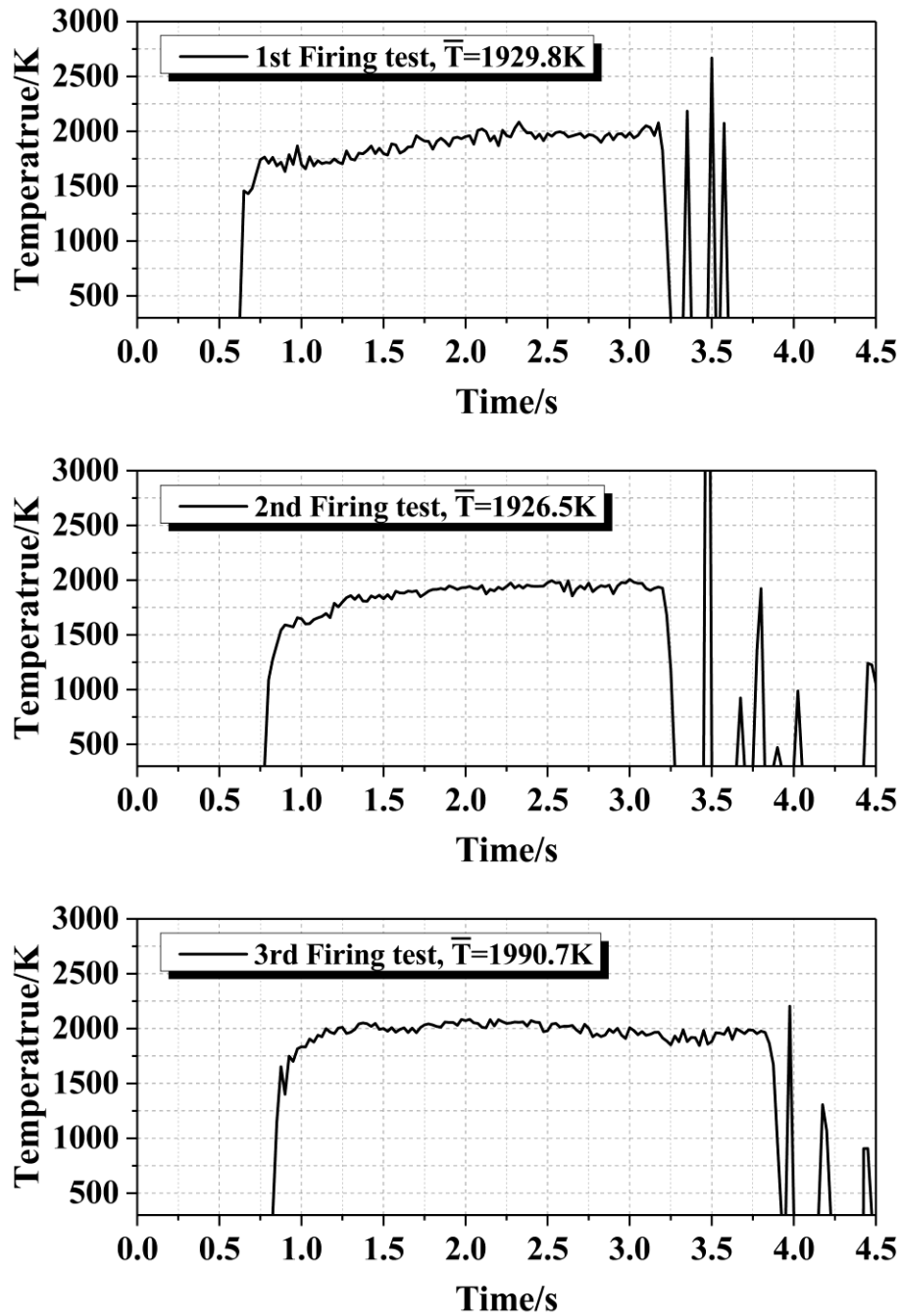


Fig.11. H₂O partial pressure results for the three firing tests.

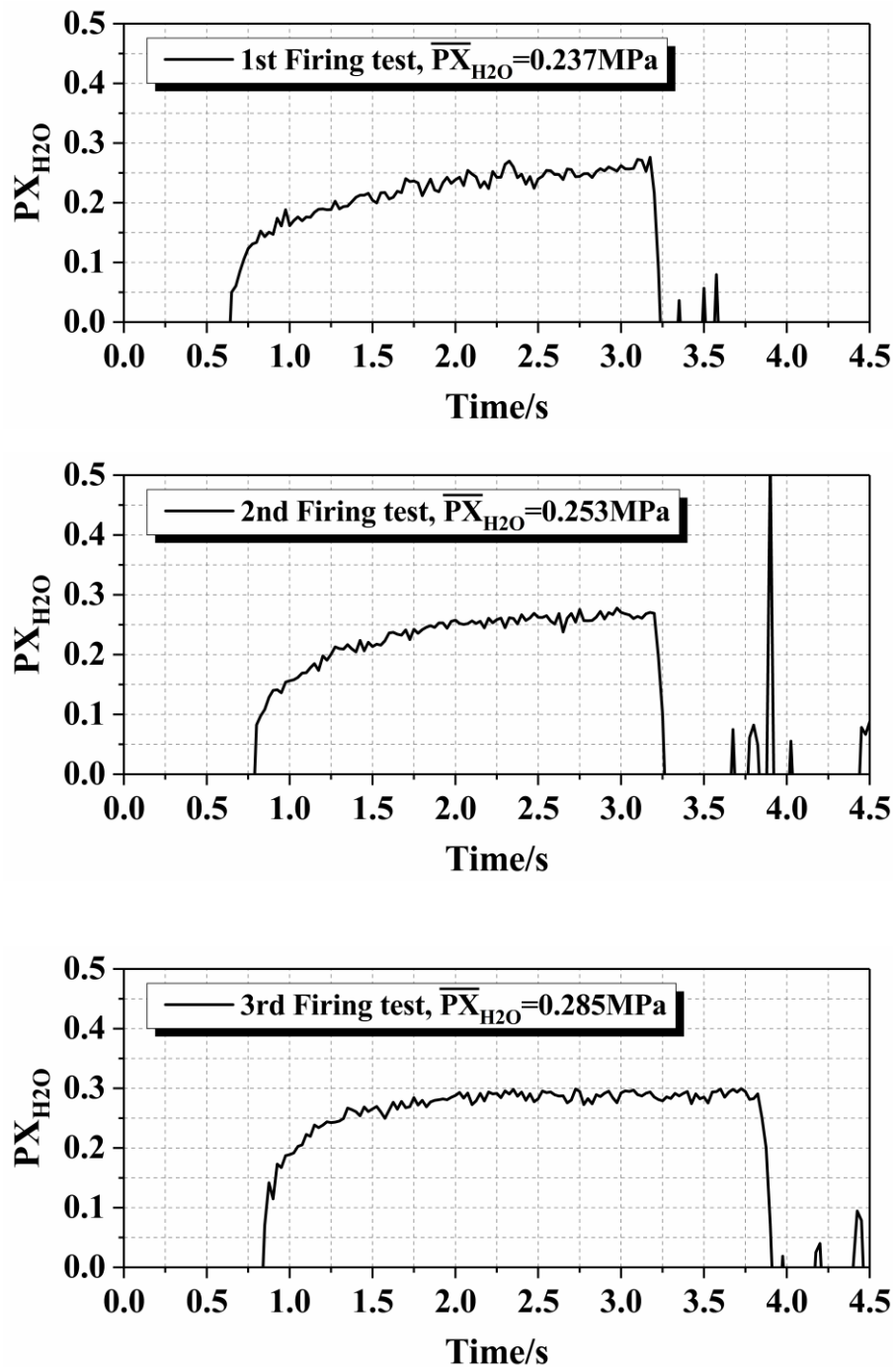


Table 1. Pertinent spectroscopic parameters for the four selected H₂O line pairs based on HITRAN 2016 database^[13].

Line Pair	Wavenumber [cm ⁻¹]	Wavelength [nm]	<i>S</i> (296K) [cm ⁻² atm ⁻¹]	<i>E</i> " [cm ⁻¹]
A ^[4]	4029.52	2481.69	8.50×10 ⁻⁵	2660.94
	4030.51	2481.08	1.80×10 ⁻⁹	4902.61
	4030.73	2480.94	2.15×10 ⁻⁹	4889.49
B ^[5]	3982.06	2511.26	8.99×10 ⁻³	1581.34
	3982.75	2510.83	6.24×10 ⁻⁷	3654.05
C ^[6]	3459.73	2890.40	4.02×10 ⁻⁶	3386.38
	3460.59	2889.68	8.85×10 ⁻⁴	2073.51
D ^[9]	3920.09	2550.96	6.49×10 ⁻¹	704.21
	4030.73	2480.94	2.15×10 ⁻⁹	4889.49